Mechanical sensors

A MEMS-Scale Ultrasonic Power Receiver for Biomedical Implants

Hamid Basaeri[1], Yuechuan Yu[2], Darrin Young[2], and Shad Roundy[1]

[1]Department of Mechanical Engineering, University of Utah, Salt Lake City, UT 84112 USA
[2]Department of Electrical and Computer Engineering, University of Utah, Salt Lake City, UT 84112 USA

Manuscript received November 27, 2018; revised February 28, 2019; accepted March 7, 2019. Date of publication March 11, 2019; date of current version April 2, 2019.

Abstract—Bio-implantable medical devices need a reliable and stable source of power to perform effectively. Although batteries are typically the first candidate to power implantable devices, they have a limited lifetime and must be periodically replaced or recharged. To alleviate this issue, ultrasonic power transfer systems can wirelessly power bio-implantable devices. Diaphragm structures which use piezoelectric materials (also known as piezoelectric micromachined ultrasonic transducers) can be fabricated on a small scale suitable for implantable devices. Diaphragms can be fabricated by deposition of lead zirconate titanate (PZT) films on a non-piezoelectric material. However, current deposition techniques cannot provide PZT thicknesses more than about 6 μm. We numerically investigate the performance of a square ultrasonic PZT receiver with inner and outer electrodes. Using COMSOL simulations, we optimize the piezoelectric film thickness for a 2 mm $\times$ 2 mm diaphragm with a silicon substrate of 50 μm and find the optimal thickness to be 20 μm for a maximum output power delivered to an optimal load. We fabricate a micromachined ultrasonic power-generating receiver capable of providing sufficient power for implantable medical devices using bulk PZT. We show that when a transmitter is generating an input power intensity of 322 mW/cm^2 at 88 kHz, less than Food and Drug Administration limit of 720 mW/cm^2, the receiver delivers a power of 0.7 mW to an optimal resistive load of 4.3 kΩ when the distance between the transmitter and the receiver is 20 mm. Furthermore, the process developed can be used to fabricate devices that are significantly smaller than the one characterized, which enables further miniaturization of bio-implanted systems.

Index Terms—Mechanical sensors, acoustic energy harvesting, acoustic power transfer, implantable sensors, piezoelectric micromachined ultrasonic transducer (pMUTs).

I. INTRODUCTION

Acoustic power transfer can be a safe alternative to batteries. In comparison to other wireless transfer methods such as inductive and radio frequency power transfer, acoustic energy has much shorter wavelengths and relatively lower attenuation in human tissue; therefore, acoustic energy can be more efficient for small devices and large implant depths. For a more detailed discussion of acoustic power transfer for implantable medical devices (IMDs), see a recent review [1]. In these systems, an external transmitter converts electrical energy into pressure wave, which is transferred through the human body. A receiver, implanted in the body, captures and converts the pressure wave to electrical energy (typically using the piezoelectric effect). A rectifier provides a usable stable dc voltage for IMDs. There are two common architectures for ultrasonic power receiver structures: plate and diaphragm architectures. Diaphragm structures have been sparsely studied [2]–[4] compared to off-the-shelf plate transducers [5]–[7]. Although the plate is the more widely used architecture, the diaphragm can be a better candidate for powering a bio-implantable device because it can be smaller at a given operating frequency and can produce more power at very small scales [8].

The majority of researchers developing piezoelectric micromachined ultrasonic transducers (pMUTs) use thin film deposition techniques such as sol-gel spin coating [9], screen printing [10], and sputtering [11]. Microelectromechanical systems (MEMS) piezo processes can only fabricate layer thicknesses up to 6 μm [12]. These thin piezo films suffer from a low electromechanical coupling coefficient due to film stresses and/or lower density compared to their bulk piezo material counterparts [13]. As an alternative to deposited piezo layers, high-quality bulk piezo materials can be used in the fabrication of pMUTs. However, off-the-shelf piezo transducers are typically 100-μm thick or thicker, which results in a large gap in available piezoelectric material thickness between deposited thin layers and off-the-shelf bulk transducers. When an ultrasound receiver requires a piezo layer with thickness between 6 and 100 μm to deliver the maximum power to an optimal load, neither of these techniques can be used.

In this article, we numerically and experimentally investigate the power generation capability of a pMUT. The magnitude of the transferred power depends on several factors including size of the receiver and the operating frequency. The pMUT needs to be small to reduce the trauma to the patient and needs to operate at a relatively low frequency ($\sim$100 kHz) to reduce attenuation in human tissue. To achieve a 2 mm $\times$ 2 mm device capable of operating in low frequencies, we study the effect of the thickness of the piezoelectric layer on the generated voltage and power. The ideal piezo thickness for that particular size and frequency combination is in the 6 to 100 μm range. Since this thickness can be provided by neither current deposition techniques nor off-the-shelf piezo transducers, we propose a fabrication process using bulk piezo materials that can bridge the gap in available piezoelectric layer thicknesses. We start with a thick bulk lead zirconate titanate (PZT) and polish it down to produce a PZT layer that is thicker than standard microfabrication processes but thin enough for a millimeter scale bending diaphragm. Then, we characterize the fabricated device in air and water and investigate the performance of the device as an acoustic power receiver.

II. DESIGN AND FABRICATION

The device structure of the proposed pMUT receiver with patterned inner and outer electrodes is illustrated in Fig. 1(a). When acoustic

Corresponding author: Hamid Basaeri (e-mail: h.basaeri@utah.edu).
Associate Editor: M. Rinaldi
Digital Object Identifier 10.1109/LSENS.2019.2904194

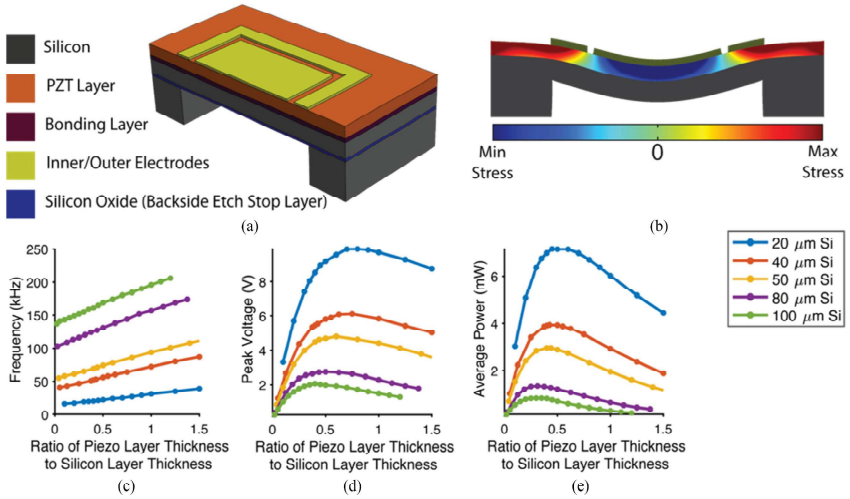

Fig. 1. (a) Schematic drawing showing the cross-sectional view of the proposed micromachined ultrasonic receiver. (b) Working principle of the pMUT structure with inner and outer electrodes; the edge of the inner electrode is placed where stress changes direction. (c) Simulated resonance frequency versus ratio of piezo thickness to silicon thickness. (d) Simulated peak voltage versus ratio of piezo thickness to silicon thickness. (e) Simulated average power across an optimal resistive load versus ratio of piezo thickness to silicon thickness.

pressure is applied to the receiver, the inner (outer) portion of the diaphragm will be in tension, whereas the outer (inner) portion will be in compression [14]. To achieve the maximum voltage, the inner electrode needs to be placed up to where the sum of stresses becomes zero [see Fig. 1(b)]. By placing inner and outer electrodes on the top surface of PZT, there is no need to access the floating bottom electrode of PZT that makes the fabrication process much easier. Our proposed electrode configuration results in a lower electrical capacitance compared to typical pMUTs with top and bottom electrodes.

When the device is subjected to acoustic pressure, the applied pressure is converted to electrical energy by the direct piezoelectric effect. The generated voltage and power depend on the thickness of the piezoelectric layer. Assuming a piezo with a thickness of t and a cross-sectional area of A is being cyclically stressed at frequency ω, the generated power dissipated through an optimal resistive load can be derived as follows [15]:

$$P_{\text{rms}} = \frac{1}{4}\omega k^2 c^E (At) S^2 \tag{1}$$

where k and c^E are the coupling coefficient and stiffness of piezo, respectively, and S is the zero-to-peak strain in the piezo. When the piezo thickness increases, the volume increases, so the power should go up; however, the strain decreases since thinner layers of piezoelectric material have higher strains. When the thickness becomes too large, the reduction in strain dominates. On the other hand, as thickness gets too low, not having enough piezo material dominates. Therefore, there is a thickness at which the power is optimized. COMSOL simulations have been carried out in water for different thickness of piezoelectric and silicon layers. The length of a side of the square receiver is set to be 2 mm, and the patterned electrodes are also modeled. At each thickness, the device is operated at its resonance frequency, and the optimal load is used for estimating the generated voltage and power. The resonance frequency, generated peak voltage, and average power are plotted against the ratio of piezo thickness to silicon thickness in Fig. 1(c)–(e), respectively. In this study, our aim is to maximize the power available for a biomedical implant of a size significantly less than 1 cm^2. Thus, we restrict ourselves to 4 mm^2 for the power receiver. Our goal is to produce the maximum amount of power within this size constraint. We desire a relatively low resonance frequency in order to minimize attenuation in tissue. However, we still need to operate well above audible frequencies. This leads us to a desired device frequency of approximately 100 kHz. The total diaphragm thickness (around 70 μm) was chosen to operate at about this frequency within a 4-mm^2 area. For this specific design, the ratio of optimal PZT thickness to silicon thickness is around 0.4, resulting in a desired silicon layer thickness of 50 μm and a PZT layer thickness of 20 μm. One could also design an array of smaller and thinner devices with the same resonance frequency and fit them in the 4-mm^2 area. Such a device could result in similar high-power levels. However, we chose to use a single larger device with thick bulk piezoelectric materials to take advantage of their better performance.

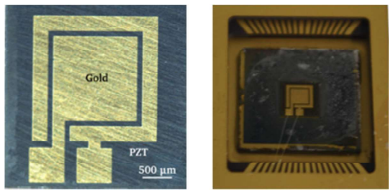

Fig. 2. (Left) Close-up of one square chip. (Right) Microfabricated PZT power receiver packaged for characterization.

The device was fabricated at the wafer-level with a silicon on insulator (SOI) wafer. The three-mask fabrication process includes deposition of bonding layer metals, bonding, mechanical lapping, release of diaphragm structure by back-side etching of the SOI wafer, and deposition of inner and outer electrodes (Cr/Au). The fabrication process starts with deposition of the bonding layer metals (Au/In) on the bulk PZT-5A and SOI wafer. The bonding layers act as a floating electrode and consist of 2.2 μm of Au and 600 nm of In on the wafer and 2.2 μm of Au on PZT. Then, the PZT sheet was diced into small square pieces of the desired size. The PZT pieces were then bonded to the SOI wafer using a heated platen press with a bonding pressure of 0.75 MPa at 188 °C for 1 h. Although there are several bonding techniques available, we chose In-Au diffusion bonding and used metals, instead of polymers, as the bonding layers in order to get a robust and high-quality bond and in order to stay well below the PZT Curie temperature of 350 °C. Gold can be used as a good bonding layer; however, the bonding temperature would be as high as 500 °C [16]. We used indium as the other bonding layer which has a relatively low melting temperature to reduce the bonding temperature. In this bonding technique, called transient-liquid-phase diffusion bonding, a low melting point interlayer metal (indium) is sandwiched in between two parent metals (gold). As the temperature increases, the molten

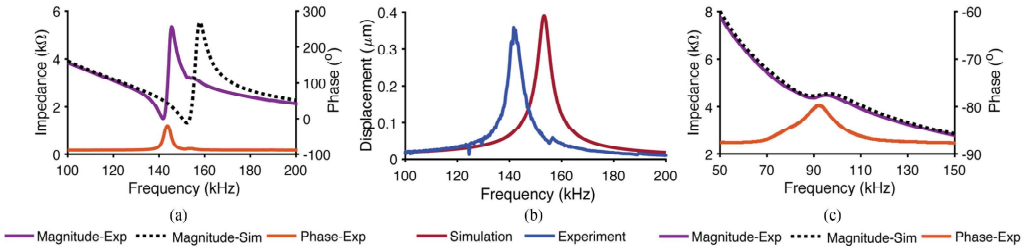

Fig. 3. (a) Impedance of the fabricated acoustic power receiver in air. (b) Comparison of measured and simulated displacement in air. (c) Impedance of the fabricated acoustic power receiver in water.

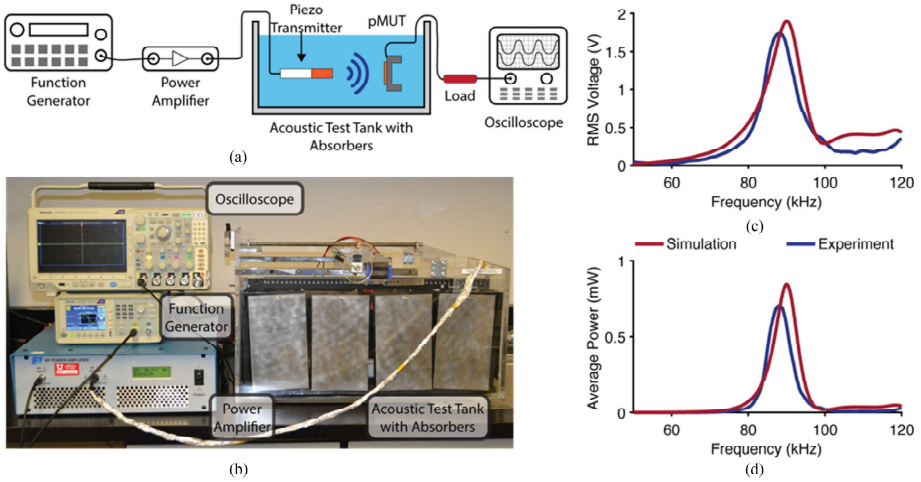

Fig. 4. (a) Schematic of the test setup for measuring voltage and power. (b) Actual test setup for measuring voltage and power. (c) Comparison of measured and simulated output voltage on a 4.3 kΩ resistive load at a distance of 20 mm in water. (d) Comparison of measured and simulated output power on a 4.3 kΩ resistive load at a distance of 20 mm in water.

interlayer diffuses into and reacts with the parent metals on both sides [17]. Mechanical lapping and polishing processes were performed to decrease the thickness of the bulk PZT from 127 to ~40 μm. (Note that we choose a higher than optimal PZT thickness as our manual polishing process is not accurate enough to guarantee 20 μm thickness, and we stopped the polishing at 40 μm since we did not want to take the risk of ending up with a thickness less than 20 μm. The thickness variation over the surface of the PZT on a single device is about ± 1 μm.) The diaphragm was created by back-side deep reactive ion etch (DRIE) stopping on a 100-nm SiO_2 layer. Finally, the top electrodes were patterned by sputtering and lifting off of Cr/Au. Fig. 2 shows photographs of the fabricated and packaged device.

III. RESULTS AND DISCUSSION

The fabricated diaphragm was first characterized in air. The impedance characterization was performed using an impedance analyzer (Agilent 4294A), as shown in Fig. 3(a). Off-resonance, the phase is $-90°$ since the device acts like a capacitor; however, at resonance the reactance is zero leaving only a real impedance and the phase goes to zero. The resonance and anti-resonance frequencies are 140.25 kHz and 145.75 kHz, respectively. The effective electromechanical coupling coefficient k_{eff}^2 can be derived from the resonance frequency f_r and the anti-resonance frequency f_a through the following relation [18]:

$$k_{eff}^2 = \frac{f_a^2 - f_r^2}{f_a^2}. \tag{2}$$

The calculated effective electromechanical coupling coefficient (k_{eff}) of the presented pMUT is 0.272, which is in line with what would be expected from a device with bulk PZT material (the published coupling coefficient of the piezoelectric material is 0.35 (k_{31}) [19]) and is significantly higher than most deposited PZT materials [20].

Actuated displacement of the fabricated device was measured using a laser Doppler vibrometer. Tests were run with a swept 3 V_{pp} sinusoidal input from a function generator (Tektronix AFG1062). Frequency sweep ranges were between 100 and 200 kHz. In order to confirm that the piezoelectric properties of the bulk material are fully conserved, measured displacement of a diaphragm is compared with its FEA simulation in Fig. 3(b). The piezoelectric layer thickness is set to 40 μm in the simulations. The experimental results agree well with the values extracted from COMSOL simulations. The measured resonance frequency of the device in air is 142 kHz, whereas the resonance frequency of the simulated device is 151 kHz. The small difference between the simulated and experimental resonance frequency values could result from not accounting for the metal layers in the simulation, and nonperfect polishing and DRIE processes. As power generation is a strong function of the quality factor (Q), it is important to empirically validate the quality factor for the MEMS implementation. The values of Q factor are used in our simulations to account for losses. The measured mechanical quality factor of the fabricated device in air is 33.8.

Second, the device was tested in an acoustic water tank. The test tank is a 59 × 28 × 28 cm^3 acrylic tank lined with ultrasoft polyurethane acoustic absorbers. Fig. 3(c) shows the impedance measurement in water and is compared to COMSOL simulations. The measured and simulated resonance frequencies in water are 88 and 90 kHz, respectively. The resonance frequency of the device decreases from 142 to 88 kHz due to the effect of added mass in water. Water has higher damping compared to air, which

lowers the Q factor. The measured Q factor of the device in water is 6.

After characterizing the device, the performance of the fabricated device in transferring power was investigated in a water-filled acoustic test tank. The schematic and image of the test setup are shown in Fig. 4(a) and (b), respectively. For the transmitter, a piezoelectric cylinder (APC Inc.; 850 material, 28.65-mm thick, 12.8 mm diameter) with a resonance frequency of 47 kHz in water was mounted to acrylonitrile-butadiene-styrene (ABS) tubing (McMaster-Carr; 1839T371) with cyanoacrylate and placed in distilled water. During the test, the receiver voltage under loading was measured and recorded for the peak input electrical power of 417.7 mW. The input power was calculated by knowing the input voltage and the impedance characteristics of the transmitter. As shown in Fig. 4(c), the device is capable of producing 1.74 V_{RMS} across an optimal load of 4.3 kΩ. The optimal load is the load at which the average power is maximum. It was selected by sweeping the resistive load and recording the voltage across the resistor. Three-dimensional COMSOL simulations were carried out by modeling the pMUT, the transmitter and the medium. Simulated and experimentally measured voltage and power of the pMUT are shown in Fig. 4(c) and (d) for the same transmitted acoustic intensity. The 1.74 V_{RMS} voltage results in average output power of 0.7 mW and a power density of 17.5 mW/cm^2. The overall efficiency of the system is about 0.33%. The input acoustic intensity of 322 mW/cm^2 is well below the safety limit for ultrasound intensity (720 mW/cm^2) defined by the United States Food and Drug Administration (FDA) [21]. The acoustic intensity at 20-mm depth is 74.8 mW/cm^2, which was measured with a hydrophone. The measured output power of 0.7 mW is significantly higher than that reported for devices with deposited PZT (59.01 μW with acoustic intensity of 700 mW/cm^2 at 10 mm [22], and 0.15 μW [23]) even with lower acoustic intensity due to the use of thicker PZT. The generated output power can be improved by applying input power intensity closer to the FDA limit and also using matching layers for the transmitter to reduce the reflection between the transmitter and the medium.

IV. CONCLUSION

In summary, a pMUT with inner and outer electrodes was developed using bulk piezoelectric materials. We found the optimal thickness ratio of the piezoelectric layer to silicon layer to achieve the maximum power from the device. We presented a fabrication process that is capable of producing piezo thicknesses much higher than current thin film deposition techniques. The fabricated device can operate at lower frequencies compared to off-the-shelf transducers resulting in lower attenuation in an aqueous environment. We characterized the device in air and water. The device is capable of providing 0.7 mW of power, which is sufficient for most bio-medical implants. As the final application of these devices is implantation in the human body, they need to be coated and packaged with bio-compatible materials [24]. Moreover, the acoustic power receiver may be misorientated at some angle with respect to the transmitter and may be laterally misaligned after being implanted in the human body. Any changes in the location of the receiver could affect the received power [25]. Future work should, therefore, include investigation of the location uncertainties on the performance of the device. This device shows great potential for powering IMDs since it can generate sufficient power in larger depth compared to other thin film receivers.

ACKNOWLEDGMENT

This work was supported by the National Science Foundation under Award ECCS 1408265.

REFERENCES

[1] H. Basaeri, D. B. Christensen, and S. Roundy, "A review of acoustic power transfer for bio-medical implants," *Smart Mater. Struct.*, vol. 25, no. 12, 2016, Art. no. 123001.

[2] Z. Wang *et al.*, "A flexible ultrasound transducer array with micro-machined bulk PZT," *Sensors*, vol. 15, no. 2, pp. 2538–2547, 2015.

[3] T. Wang, T. Kobayashi, and C. Lee, "Micromachined piezoelectric ultrasonic transducer with ultra-wide frequency bandwidth," *Appl. Phys. Lett.*, vol. 106, no. 1, 2015, Art. no. 013501.

[4] Q. Shi, T. Wang, and C. Lee, "MEMS based broadband piezoelectric ultrasonic energy harvester (PUEH) for enabling self-powered implantable biomedical devices," *Sci. Rep.*, vol. 6, 2016, Art. no. 24946.

[5] T. C. Chang, M. J. Weber, M. L. Wang, J. Charthad, B. T. Khuri-Yakub, and A. Arbabian, "Design of tunable ultrasonic receivers for efficient powering of implantable medical devices with reconfigurable power loads," *IEEE Trans. Ultrason. Ferroelect. Freq. Control*, vol. 63, no. 10, pp. 1554–1562, Oct. 2016.

[6] H. Basaeri, D. Christensen, Y. Yu, T. Nguyen, P. Tathireddy, and D. J. Young, "Ultrasonically powered hydrogel-based wireless implantable glucose sensor," in *Proc. IEEE Sens.*, 2016, pp. 1–3.

[7] D. Seo, J. M. Carmena, J. M. Rabaey, M. M. Maharbiz, and E. Alon, "Model validation of untethered, ultrasonic neural dust motes for cortical recording," *J. Neuroscience Methods*, vol. 244, pp. 114–122, 2015.

[8] D. B. Christensen and S. Roundy, "Ultrasonically powered piezoelectric generators for bio-implantable sensors: Plate versus diaphragm," *J. Intell. Mater. Syst. Struct.*, vol. 27, no. 8, pp. 1092–1105, 2016.

[9] L. Pardo, R. Jiménez, A. García, K. Brebøl, G. Leighton, and Z. Huang, "Impedance measurements for determination of elastic and piezoelectric coefficients of films," *Adv. Appl. Ceram.*, vol. 109, no. 3, pp. 156–161, 2010.

[10] C. G. Hindrichsen, R. Lou-Moller, K. Hansen, and E. V. Thomsen, "Advantages of PZT thick film for MEMS sensors," *Sens. Actuators, A Phys.*, vol. 163, no. 1, pp. 9–14, 2010.

[11] E. Mehdizadeh and G. Piazza, "Through-package wireless powering via piezoelectric micromachined ultrasonic transducers," in *Proc. IEEE Int. Conf. Micro Electro Mech. Syst.*, 2018, pp. 1076–1079.

[12] C. Cassella and G. Piazza, "AlN two-dimensional-mode resonators for ultra-high frequency applications," *IEEE Electron Device Lett.*, vol. 36, no. 11, pp. 1192–1194, Nov. 2015.

[13] S. Trolier-Mckinstry and P. Muralt, "Thin film piezoelectrics for MEMS," *J. Electroceramics*, vol. 12, pp. 7–17, 2004.

[14] S. Kim, W. W. Clark, and Q. Wang, "Piezoelectric energy harvesting using a diaphragm structure," *Smart Struct. Mater.*, vol. 5055, pp. 307–318, 2003.

[15] X. Ma, A. Wilson, C. D. Rahn, and S. Trolier-McKinstry, "Efficient energy harvesting using piezoelectric compliant mechanisms: Theory and experiment," *J. Vib. Acoust.*, vol. 138, no. 2, 2016, Art. no. 021005.

[16] K. Tanaka, T. Konishi, M. Ide, and S. Sugiyama, "Wafer bonding of lead zirconate titanate to Si using an intermediate gold layer for microdevice application," *J. Micromechanics Microeng.*, vol. 16, no. 4, pp. 815–820, 2006.

[17] E. E. Aktakka, R. L. Peterson, and K. Najafi, "Wafer-level integration of high-quality bulk piezoelectric ceramics on silicon," *IEEE Trans. Electron Devices*, vol. 60, no. 6, pp. 2022–2030, Jun. 2013.

[18] J. Jung, S. Kim, W. Lee, and H. Choi, "Fabrication of a two-dimensional piezoelectric micromachined ultrasonic transducer array using a top-crossover-to-bottom structure and metal bridge connections," *J. Micromechanics Microeng.*, vol. 23, no. 12, 2013, Art. no. 125037.

[19] "PSI-5A4E Piezoceramic Sheets and Their Properties, Piezo Systems, Inc." [Online]. Available: http://www.piezo.com/prodsheet1sq5A.html

[20] P. Muralt *et al.*, "Piezoelectric micromachined ultrasonic transducers based on PZT thin films," *IEEE Trans. Ultrason. Ferroelect. Freq. Control*, vol. 52, no. 12, pp. 2276–2288, Dec. 2005.

[21] "Guidance for industry and FDA staff information for manufacturers seeking marketing clearance of diagnostic ultrasound systems and transducers," FDA, Silver Spring, MD, USA, 2008.

[22] Q. Shi, T. Wang, T. Kobayashi, and C. Lee, "Investigation of geometric design in piezoelectric microelectromechanical systems diaphragms for ultrasonic energy harvesting," *Appl. Phys. Lett.*, vol. 108, no. 19, pp. 106–111, 2016.

[23] B.-S. Lee, P.-J. Shih, J.-J. He, W.-P. Shih, and W.-J. Wu, "A study of implantable power harvesting transducers," *Proc. SPIE*, vol. 6530, 2007, Art. no. 65300I.

[24] C. Zhang, T. W. Piaget, K. R. Maile, and R. A. Balczewski, "Acoustic communication transducer in implantable medical device header," U.S. Patent 570,998B2, 2002.

[25] D. B. Christensen, H. Basaeri, and S. Roundy, "A computationally efficient technique to model depth, orientation and alignment via ray tracing in acoustic power transfer systems," *Smart Mater. Struct.*, vol. 2006, no. 12, 2017, Art. no. 125020.